

# Dosemetric Parameters Predictive of Rib Fractures after Proton Beam Therapy for Early-Stage Lung Cancer

Yojiro Ishikawa,<sup>1</sup> Tatsuya Nakamura,<sup>2</sup> Takahiro Kato,<sup>2</sup> Noriyuki Kadoya,<sup>1</sup> Motohisa Suzuki,<sup>2</sup> Yusuke Azami,<sup>2</sup> Masato Hareyama,<sup>2</sup> Yasuhiro Kikuchi<sup>2</sup> and Keiichi Jingu<sup>1</sup>

<sup>1</sup>Department of Radiation Oncology, Tohoku University Graduate School of Medicine, Sendai, Miyagi, Japan

<sup>2</sup>Department of Radiation Oncology, Southern Tohoku Proton Therapy Center, Southern Tohoku Research Institute for Neuroscience, Koriyama, Fukushima, Japan

Proton beam therapy (PBT) is the preferred modality for early-stage lung cancer. Compared with X-ray therapy, PBT offers good dose concentration as revealed by the characteristics of the Bragg peak. Rib fractures (RFs) after PBT lead to decreased quality of life for patients. However, the incidence of and the risk factors for RFs after PBT have not yet been clarified. We therefore explored the relationship between irradiated rib volume and RFs after PBT for early-stage lung cancer. The purpose of this study was to investigate the incidence and the risk factors for RFs following PBT for early-stage lung cancer. We investigated 52 early-stage lung cancer patients and analyzed a total of 215 irradiated ribs after PBT. Grade 2 RFs occurred in 12 patients (20 ribs); these RFs were symptomatic without displacement. No patient experienced more severe RFs. The median time to grade 2 RFs development was 17 months (range: 9-29 months). The three-year incidence of grade 2 RFs was 30.2%. According to the analysis comparing radiation dose and rib volume using receiver operating characteristic curves, we demonstrated that the volume of ribs receiving more than 120 Gy<sub>3</sub> (relative biological effectiveness (RBE)) was more than 3.7 cm<sup>3</sup> at an area under the curve of 0.81, which increased the incidence of RFs after PBT (P < 0.001). In this study, RFs were frequently observed following PBT for early-stage lung cancer. We demonstrated that the volume of ribs receiving more than 120 Gy<sub>3</sub> (RBE) was the most significant parameter for predicting RFs.

**Keywords:** Bragg peak; early-stage lung cancer; proton beam therapy; rib fracture; stereotactic radiotherapy  
Tohoku J. Exp. Med., 2016 April, 238 (4), 339-345. © 2016 Tohoku University Medical Press

## Introduction

Lung cancer is associated with a high mortality rate in Japan (Matsuda et al. 2013). Local surgery is the standard treatment for early-stage non-small-cell lung cancer (NSCLC). On the other hand, small-cell lung cancer is characterized by the early development of widespread metastases; therefore, with a few exceptions, local surgery is not the standard treatment. Stereotactic radiotherapy (SRT) is the established treatment for early-stage lung cancer that is inoperable because of medical contraindications, and it achieves good local control (McGarry et al. 2005; Nagata et al. 2005; Timmerman et al. 2006; Baumann et al. 2009; Shirata et al. 2012). However, desired dose applications within target volumes are limited because of the proximity to critical normal tissues. Also, the incidence of rib fractures (RFs) following SRT for early-stage lung cancer ranges from 4% to 37.7% (Pettersson et al. 2009; Dunlap et

al. 2010; Andolino et al. 2011; Welsh et al. 2011; Asai et al. 2012; Creach et al. 2012; Mutter et al. 2012; Stephans et al. 2012; Taremi et al. 2012; Nambu et al. 2013).

Compared with X-ray therapy, proton beam therapy (PBT) offers good dose concentration, as revealed by the characteristics of the Bragg peak, and provides advantages over SRT in terms of decreasing doses to normal tissues as well as in treating early-stage NSCLC (Georg et al. 2008; Kadoya et al. 2011). Kanemoto et al. (2013) discussed RF following PBT for peripheral hepatocellular carcinomas, excluding central lesions, which were treated with 66 cobalt Gy equivalents [Gy; relative biological effectiveness (RBE)] in 10 fractions. In early-stage lung cancer with central lesions, critical organs, such as the esophagus, gastrointestinal tract, and heart, often impose limitations on the prescribed dose to a target volume. Therefore, the following tumor location-dependent prescribed doses are used for early-stage lung cancers in the Southern Tohoku Proton

Received October 22, 2015; revised and accepted March 22, 2016. Published online April 15, 2016; doi: 10.1620/tjem.238.339.

Correspondence: Yojiro Ishikawa, Department of Radiation Oncology, Tohoku University Graduate School of Medicine, 1-1 Seiryomachi, Aoba-ku, Sendai, Miyagi 980-8574, Japan.  
e-mail: y02614111@yahoo.co.jp

Therapy Center (STPTC): 66 Gy (RBE) in 10 fractions and 80 Gy (RBE) in 25 fractions.

PBT-induced RF is a clinical complication that occurs in patients with early-stage lung cancer and hepatocellular carcinoma. The risk factors and dose parameters for RFs have been analyzed in several previous studies (Taremi et al. 2012; Nambu et al. 2013). However, little is known regarding RFs following PBT, which often cause prolonged pain, long-term disability, and a decreased quality of life (Richardson et al. 2007; Nirula and Mayberry 2010; Kanemoto et al. 2013). Therefore, in the current study, we investigated the cumulative incidence and dose-volume responses of RFs following PBT for early-stage lung cancer.

## Materials and Methods

### Patients

Between January 2009 and January 2012, 52 early-stage lung cancer patients (33 males, 19 females) with stage I NSCLC were treated with PBT at STPTC (Table 1). The study was approved by the research and ethics committee of STPTC. The authors conformed to the ethical guidelines of the 1975 Declaration of Helsinki (revised in 2000). The median age at treatment was 78 years (range: 61-89 years). Histological cancer types were adenocarcinoma (n = 26; 50%), squamous cell carcinoma (n = 10; 19.2%), bronchioloalveolar carcinoma (n = 3; 5.8%), and "not otherwise specified" (n = 13; 25%). Eastern Cooperative Oncology Group performance status was 0 for 36 patients, 1 for 12 patients, and 2 for 4 patients. Twenty-seven lesions (51.9%) were treated with 66 Gy (RBE) in 10 fractions, and 25 lesions (48.1%) were treated with 80 Gy (RBE) in 25 fractions.

### Treatment protocols

We used two tumor location-dependent protocols for early-stage lung cancer: 66 Gy (RBE) in 10 fractions and 80 Gy (RBE) in 25 fractions. The first protocol, 66 Gy (RBE) in 10 fractions, was applied to peripheral tumors that were not adjacent to the esophagus, gastrointestinal tract, or heart. The second protocol, 80 Gy (RBE) in 25 fractions, was used for tumors located near the proximal bronchial tree, esophagus, or heart (Fig. 1). For this study, the proton-equivalent dose was defined as the physical dose (Gy)  $\times$  1.1 RBE. The equivalent dose was calculated using a linear quadratic equation. Because different fractionation schemes were used for patients examined in this study, we used the biologically effective dose (BED) rather than the physical dose. The BED was calculated by

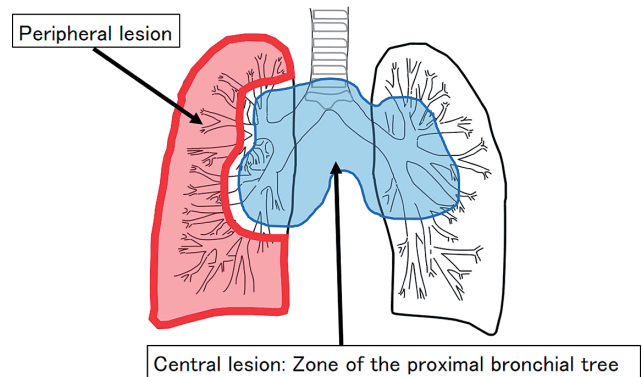


Fig. 1. Images of central and peripheral lesions.

A dose of 66 Gy (RBE) in 10 fractions was used for peripheral tumors. A dose of 80 Gy (RBE) in 25 fractions was used when the tumor was located near the proximal bronchial tree.

Table 1. Patient and tumor characteristics.

	N or range	% or median
No. of patients	52	100%
Age (years)	61-89	78
Male/Female	33/19	63.5/36.5
Right/Left	21/31	40.4/59.6
PBT Method		
66 Gy (RBE)/10 fractions	27	51.9%
80 Gy (RBE)/25 fractions	25	48.1%
T1a/T1b/T2a	20/19/13	38.5/36.5/25
Stage 1A/1B	39/13	75/25
AC/SCC/BAC/GGO	26/10/3/13	50/19.2/5.8/25
Peripheral/Central	41/11	78.8/21.2
Tumor size (mm)	10-48	24.5
Tumor-rib distance (mm)	0-63	3.0

AC, adenocarcinoma; SCC, squamous cell carcinoma; BAC, bronchioloalveolar carcinoma; GGO, ground-glass opacity.

$$\text{BED} = nd [1 + d/(\alpha/\beta)]$$

where  $n$  was the number of fractions and  $d$  was the dose/fraction. The  $\alpha/\beta$  tumor ratio was set at 10 Gy. Late-responding tissue was assigned an  $\alpha/\beta = 3$  Gy. BEDs for 66 Gy in 10 fractions and 80 Gy in 25 fractions calculated with an  $\alpha/\beta = 10$  Gy were 110 and 106 Gy<sub>10</sub> (RBE), respectively. A BED with an  $\alpha/\beta = 3$  Gy was used to determine the radiation dose to ribs [Gy<sub>3</sub> (RBE)]. Dose-volume histogram (DVH) parameters used were as follows: V100, volume of rib receiving > 100 Gy<sub>3</sub> (RBE); V120, volume receiving > 120 Gy<sub>3</sub> (RBE); V140, volume receiving > 140 Gy<sub>3</sub> (RBE); V160, volume receiving > 160 Gy<sub>3</sub> (RBE); and V180, volume receiving > 180 Gy<sub>3</sub> (RBE). In addition, relationships were determined for RFs incidence and the maximum dose ( $D_{\max}$ ) Gy<sub>3</sub> (RBE) to irradiated ribs.

#### Proton delivery system

The PBT system (Mitsubishi Electric Corp., Tokyo, Japan) used in the STPTC has a synchrotron that can accelerate protons up to 235 MeV. This system uses a passive scattering method wherein a proton beam passes through a bar ridge filter, a range shifter, and a customized compensator before entering a patient. The wobblers system is comprised of two dipole magnets, and scattering elements create a broad, flattened beam at the final aperture. A bar ridge filter is combined with this system to produce a three-dimensional, uniformly spread Bragg peak. The spread out Bragg peak widths were used 30, 40, 50, 60, 70, 80, 90, 100, 110 and 120 mm. The multi-leaf collimator is comprised of 40 3.75-mm-wide iron plates. These plates can be molded into any irregular shape. A range shifter is used to determine the maximum proton penetration depth, and the customized compensator is used to confirm the dose to the distal edge of the target.

#### Treatment planning

A commercial treatment planning system (XiO-M; Elekta, Stockholm, Sweden/Mitsubishi Electric Corp.) was used to calculate dose distributions for PBT. PBT was planned using a pencil beam algorithm (Hong et al. 1996; Akagi et al. 2006). The normalization point (100%) was defined as the center of the planning target volume (PTV). The exhalation phase, determined by respiration-gated computed tomography (CT), was used in our treatment plan. The respiratory phase was monitored with abdominal wall movements. The gross tumor volume contours were manually outlined on serial lung-window CT images. The clinical target volume was defined as gross tumor volume with a 5-mm margin in all directions. The clinical target volume was expanded by 5 mm in all directions for set-up uncertainty, and an additional 5-10-mm margin to create PTV was included in caudal axes to compensate for uncertainty due to respiration-induced tumor movements. Beam shapes were optimized using the multi-leaf collimator.

Ribs to be irradiated by proton beams were contoured during treatment-planning CT. The air gap was 10 cm, and the proton beam incidence was restricted to two directions. Two proton beam energy levels, 150 and 210 MeV, were determined with the depths of distal and proximal edges of a target. Distal, proximal, and smearing margins were fundamentally calculated using Strategy 2 as reported previously (Moyers et al. 2001). Treatment parameters were adjusted according to PTV coverage and organ-at-risk position. For PTV planning, the beam incidence for PBT was restricted to two to three directions.

#### Pretreatment assessment and follow-up

All patients underwent fluorodeoxyglucose positron emission tomography before treatment as part of their staging. Follow-up evaluations were conducted at intervals of 1-3 months during the first year and every 6 months thereafter. RF was assessed by follow-up chest radiography or CT.

#### Toxicity scoring

Late rib toxicity was scored using the Common Terminology Criteria for Adverse Events, version 4.0. Briefly, asymptomatic patients with radiographic findings alone were considered as grade 1. Symptomatic patients without displacement were considered as grade 2. Symptomatic patients with displacement or open wounds with bone exposure that required surgical intervention were considered as grade 3. Grade-2 rib toxicity did not include chest wall pain due to myositis and neuralgia without RFs.

#### Statistical analysis

Our primary end point was grade 2 rib toxicity. Complication rates were determined from Kaplan-Meier estimates. Clinical variables were assessed by univariate analyses (log-rank test). Receiver operating characteristic (ROC) curves were generated to derive dose-volume constraints from retrospective clinical data. For this study, ROC curves were used to determine optimal DVH cut-off values for predicting RFs. Patients were categorized into groups above and below these optimal cut-off values. Statistical analyses were performed using the JMP software, version 10 (SAS Institute Inc., Cary, NC, USA). A P-value of < 0.05 was considered significant.

## Results

#### Incidence of RFs

Patient follow-up periods ranged from 11 to 50 months (median: 33). Data for 52 patients with a total of 215 irradiated ribs were available for analysis. Grade 2 RFs occurred in 12 (23.1%) patients (20 ribs). No patient experienced grade 3 or 4 RFs. The median time to grade 2 RFs development was 17 months (range: 9-29 months). RFs appeared no earlier than 9 months after initiating PBT. Fig. 2 shows PBT dose distributions for NSCLC and RFs following PBT.

The 3-year cumulative incidence of grade 2 RFs was 30.2% (95% confidence interval: 14.952.1%; Fig. 3). Grade 2 RFs occurred in 5 (9.6%) patients who were treated with 66 Gy (RBE) in 10 fractions and in 7 patients (13.5%) who were treated with 80 Gy (RBE) in 25 fractions. Kaplan-Meier curves for 66 and 80 Gy (RBE) revealed no significant difference with regard to grade 2 RFs ( $P > 0.05$ ; Fig. 4).

#### Dose-volume relationships

Rib contours were manually outlined on serial bone-window CT images. We did not contour cartilage. DVH was calculated for each irradiated rib as determined by treatment-planning CT.

Table 2 presents dose-volume parameters and each optimal cut-off point obtained using ROC curve analysis. Areas under the curve from ROC plots for V100, V120,

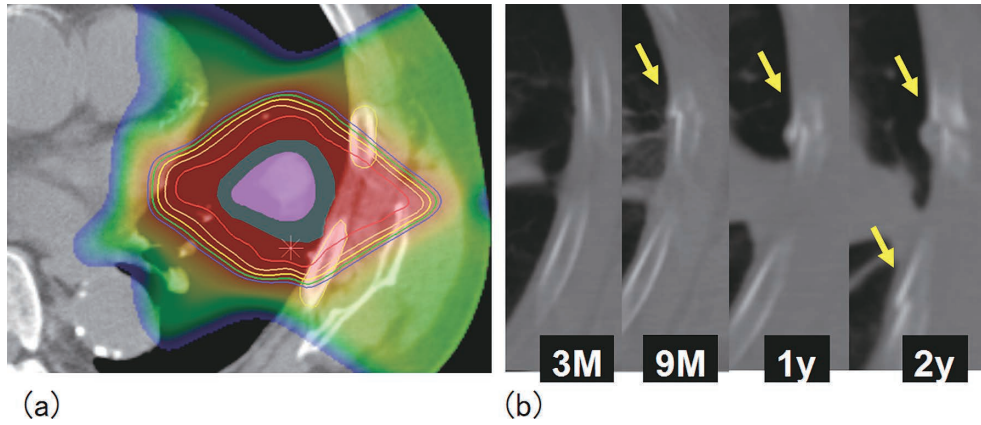


Fig. 2. Dose distribution and rib fractures.

Comparisons of proton beam therapy (PBT) dose distributions in a patient with non-small cell lung cancer (a) and rib fractures following PBT (b).

(b) Axial CT slice shows the rib fracture (arrows). This patient received 80 Gy (RBE) in 25 fractions. The rib fracture was observed at 9 months after PBT.

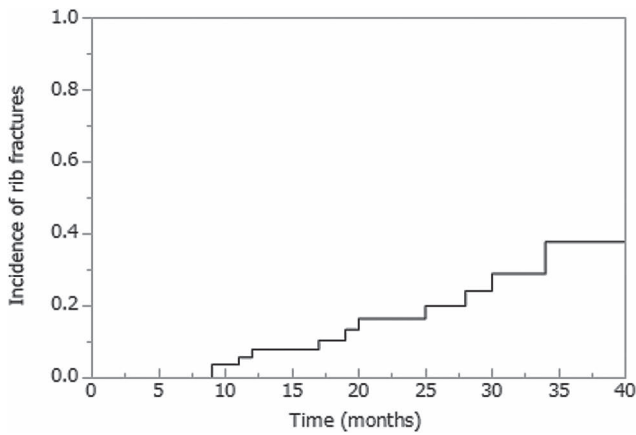


Fig. 3. Cumulative incidence of rib fractures.

Cumulative incidence of rib fractures following proton beam therapy for nonsmall cell lung cancer.

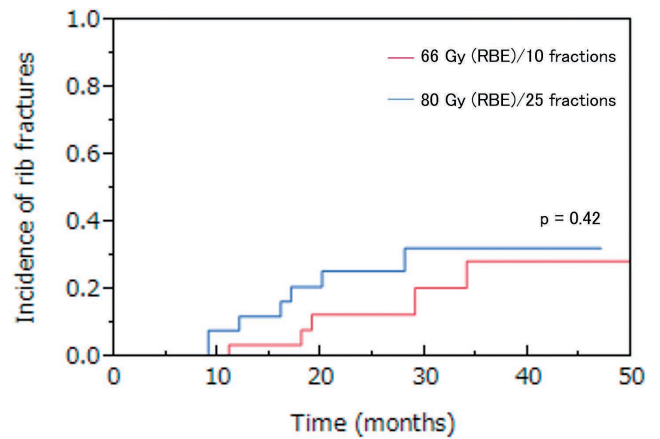


Fig. 4. Cumulative incidence of rib fractures, 66 Gy (RBE) and 80 Gy (RBE).

Cumulative incidences of rib fractures for 66 Gy (RBE) in 10 fractions and 80 Gy (RBE) in 25 fractions following proton beam therapy for nonsmall cell lung cancer.

Table 2. Comparison of the probability of radiation-induced rib fracture for each dosimetric parameter.

	AUC	Cut-off	P value (log-rank)
V100	0.78	4.7 cm <sup>3</sup>	< 0.001*
V120	0.81	3.7 cm <sup>3</sup>	< 0.001*
V140	0.80	3.4 cm <sup>3</sup>	< 0.001*
V160	0.79	1.1 cm <sup>3</sup>	< 0.001*
V180	0.53	0.07 cm <sup>3</sup>	0.59
D <sub>max</sub>	0.73	160 Gy <sub>3</sub> (RBE)	< 0.001*

AUC, area under the curve; RBE, relative biological effectiveness.

\*Significant values P < 0.05.



V140, V160, V180 and  $D_{\max}$  were 0.78, 0.81, 0.80, 0.79, 0.53 and 0.73, respectively, and all P-values were  $< 0.05$ . Optimal cut-off point values corresponded to the highest peaks on each ROC plot and were as follows: V100 = 4.7 cm<sup>3</sup>, V120 = 3.7 cm<sup>3</sup>, V140 = 3.4 cm<sup>3</sup>, and V160 = 1.1 cm<sup>3</sup>, with  $D_{\max} = 160 \text{ Gy}_3$  (RBE). This demonstrated that the greatest area under the curve was found for V120, and the optimal cut-off point was 3.7 cm<sup>3</sup>.

### Discussion

SRT and particle therapy (with proton and carbon-ion beams) have both been used to treat early-stage NSCLC. RFs are late radiotoxicity-related complication. In our study, grade 2 RFs occurred in 12 patients following PBT (19.4%), with a three-year cumulative incidence rate of 30.2%. With regard to SRT, several groups reported RFs frequencies ranging from 4% to 37.7% after SRT for early-stage NSCLC; these rates were not much higher compared with those observed in our study (30.2%) (Pettersson et al. 2009; Dunlap et al. 2010; Andolino et al. 2011; Welsh et al. 2011; Asai et al. 2012; Creach et al. 2012; Mutter et al. 2012; Stephans et al. 2012; Taremi et al. 2012; Nambu et al. 2013). Although PBT reportedly offers advantages over SRT, it has not been reported to dramatically reduce RFs incidence (Georg et al. 2008; Kadoya et al. 2011).

Some studies on SRT have reported a greater decrease in RF incidence than that observed in our study (Stephans et al. 2012; Taremi et al. 2012; Nambu et al. 2013). One reason for such differences between PBT and SRT is that the former may yield higher entrance doses compared with the latter, because of the smaller number of beams involved in PBT. Generally, two or three beams are used during PBT for lung cancer treatment because using fewer beams reduces the irradiation of normal tissue (i.e., lung tissue) and an excessive amount of time is needed to create the customized compensator required for each beam to achieve a distal PTV dose conformity in passively scattered PBT. Thus, increasing the number of beams and other irradiating techniques (layer-stacking and spot-scanning methods) may improve the high entrance dose (Kanai et al. 2006; Arjomandy et al. 2009). However, additional research is needed to resolve this issue.

With regard to PBT for other areas, Kanemoto and coworkers (2013) reported a five-year cumulative RFs incidence of 22% in 67 patients with hepatocellular carcinoma treated with PBT. The RF incidence in that study was lower than that in our study possibly because the radiation exposure associated with hepatocellular carcinoma was limited to the lower right ribs. In addition, the possible complications differ between patients with hepatocellular carcinoma and those with lung cancer. Pulmonary complications, such as chronic cough or respiratory discomfort, may increase the risk of RFs following PBT. Hanak et al. (2005) reported that cough-induced RFs primarily occurred in females with chronic cough. Several underlying mechanisms for cough-induced RFs have been speculated on. A

strong bending force during chronic coughing may cause RFs. Moreover, shearing forces generated by the serratus anterior and external oblique muscles may also be a cause.

With regard to conventional radiotherapy, Emami et al. (1991) suggested that a tolerance dose of 5/5 (tolerance dose resulting in toxicity in 5% of patients at five years) and 50/5 for partially irradiated rib cages were 50 and 65 Gy, respectively. In that study, BEDs for 50 and 65 Gy calculated with  $\alpha/\beta = 3 \text{ Gy}$  were 83 and 108 Gy<sub>3</sub> (RBE), respectively; these values were lower than our results for V120 with PBT. Using ROC curves for dosimetric parameters with SRT, Asai et al. (2012) evaluated doses administered to 374 ribs and reported a 3-year fracture rate of 37.7%. Further, they reported that  $D_{\max}$ , V40, V30, and V20 were significantly higher in fractured ribs than in non-fractured ribs. BEDs for 40, 30, and 20 Gy calculated with  $\alpha/\beta = 3 \text{ Gy}$  were 200, 150, and 100 Gy<sub>3</sub> (RBE), respectively. Compared with our results, V120 was included in these results with SRT.

However, our results indicated no relationships with high-dose regions because PBT does not yield a dose as high as  $> 200 \text{ Gy}_3$  (RBE). Therefore, with PBT, this moderate dose may be more important than a high dose for predicting RF incidence. In addition, Kanemoto et al. (2013) reported that V60 was the most significant parameter following hypofractionated PBT for hepatocellular carcinoma. Their dose-volume parameter was lower than that in our study on NSCLC.

Low-dose regions may be related to RFs following PBT for hepatocellular carcinoma. The reasons for the differences in RF DVHs between hepatocellular carcinoma and NSCLC may include tumor location and prescribed dose. Furthermore, the study by Kanemoto only included patients with peripheral hepatocellular carcinoma who underwent PBT with 66 Gy (RBE) in 10 fractions (Kanemoto et al. 2013). However, the converse is observed in patients with primary lung cancer associated with central lesions. Therefore, several prescribed doses are necessary to treat NSCLC (McGarry et al. 2005; Nagata et al. 2005; Timmerman et al. 2006; Xia et al. 2006; Baumann et al. 2009; Shirata et al. 2012).

The current study had several limitations. The median follow-up period of 33 months may have been too short to make definitive statements regarding late toxicities. Johansson et al. (2002) reported that late radiation-induced reactions often occurred after  $> 90$  days (typical range: 0.5-5 years). Furthermore, we did not identify an association between grade 2 RFs and the clinical factors that were evaluated. Patient characteristics may be associated with RFs incidence. With regard to SRT, several groups have reported that age and other patient characteristics are associated with RFs incidence. Taremi et al. (2012) reported that among 46 consecutive patients, age and female gender were significantly associated with RF. In contrast, Stephans et al. (2012) reported that no patient characteristics were predictive of toxicity, including age, body mass index, or

the presence of diabetes/hypertension/peripheral vascular disease, although current smoking status revealed an association. Nambu et al. (2013) reported smaller tumor-chest wall distance as a significant risk factor for RFs following SRT.

Another important factor that affects the incidence of late RFs is the accuracy of the dose calculations. In our study, the dose-volume parameters were examined for pencil beams. This method is frequently used by proton therapy centers. In a pencil beam dose calculation, patient's CT images are used as the model, and the patient is remapped with fluids of varying densities that are converted from CT values for individual voxels. Therefore, differences between these fluids and actual tissues may yield errors with regard to scattering power. Jiang et al. (2007) used a Monte Carlo algorithm to demonstrate this difference. Furthermore, Paganetti et al. (2008) found differences between a Monte Carlo algorithm and pencil beam calculations and these differences depended on the presence of air-bone-tissue interfaces. It may be necessary to verify uncertainties of these differences using a Monte Carlo algorithm.

RFs are frequently observed following PBT for early-stage lung cancer. DVH parameters are useful for predicting the incidence of RFs after PBT. In this study, we determined that the volume of a rib that received a BED > 120 Gy<sub>3</sub> (RBE) [V120], which had a cut-off point of 3.7 cm<sup>3</sup>, was the most significant parameter.

### Conflict of Interest

The authors declare no conflict of interest.

### References

- Akagi, T., Kanematsu, N., Takatani, Y., Sakamoto, H., Hishikawa, Y. & Abe, M. (2006) Scatter factors in proton therapy with a broad beam. *Phys. Med. Biol.*, **51**, 1919-1928.
- Andolino, D.L., Forquer, J.A., Henderson, M.A., Barriger, R.B., Shapiro, R.H., Brabham, J.G., Johnstone, P.A.S., Cardenas, H.R. & Fakiris, A.J. (2011) Chest wall toxicity after stereotactic body radiotherapy for malignant lesions of the lung and liver. *Int. J. Radiat. Oncol. Biol. Phys.*, **80**, 692-697.
- Arjomandy, B., Sahoo, N., Cox, J., Lee, A. & Gillin, M. (2009) Comparison of surface doses from spot scanning and passively scattered proton therapy beams. *Phys. Med. Biol.*, **54**, N295-N302.
- Asai, K., Shioyama, Y., Nakamura, K., Sasaki, T., Ohga, S., Nonoshita, T., Yoshitake, T., Ohnishi, K., Terashima, K., Matsumoto, K., Hirata, H. & Honda, H. (2012) Radiation-induced rib fractures after hypofractionated stereotactic body radiation therapy: risk factors and dose-volume relationship. *Int. J. Radiat. Oncol. Biol. Phys.*, **84**, 768-773.
- Baumann, P., Nyman, J., Hoyer, M., Wennberg, B., Gagliardi, G., Lax, I., Drugge, N., Ekberg, L., Friesland, S., Johansson, K.A., Lund, J.A., Morhed, E., Nilsson, K., Levin, N., Paludan, M., et al. (2009) Outcome in a prospective phase II trial of medically inoperable stage I non-small-cell lung cancer patients treated with stereotactic body radiotherapy. *J. Clin. Oncol.*, **27**, 3290-3296.
- Creach, K.M., El Naqa, I., Bradley, J.D., Olsen, J.R., Parikh, P.J., Drzymala, R.E., Bloch, C. & Robinson, C.G. (2012) Dosimetric predictors of chest wall pain after lung stereotactic body radiotherapy. *Radiother. Oncol.*, **104**, 23-27.
- Dunlap, N.E., Cai, J., Biedermann, G.B., Yang, W., Benedict, S.H., Sheng, K., Schefter, T.E., Kavanagh, B.D. & Larner, J.M. (2010) Chest wall volume receiving >30 Gy predicts risk of severe pain and/or rib fracture after lung stereotactic body radiotherapy. *Int. J. Radiat. Oncol. Biol. Phys.*, **76**, 796-801.
- Emami, B., Lyman, J., Brown, A., Cola, L., Goitein, M., Munzenrider, J.E., Shank, B., Solin, L.J. & Wesson, M. (1991) Tolerance of normal tissue to therapeutic irradiation. *Int. J. Radiat. Oncol. Biol. Phys.*, **21**, 109-122.
- Georg, D., Hillbrand, M., Stock, M., Dieckmann, K. & Pötter, R. (2008) Can protons improve SBRT for lung lesions? Dosimetric considerations. *Radiother. Oncol.*, **88**, 368-375.
- Hanak, V., Hartman, T.E. & Ryu, J.H. (2005) Cough-induced rib fractures. *Mayo Clin. Proc.*, **80**, 879-882.
- Hong, L., Goitein, M., Bucciolini, M., Comiskey, R., Gottschalk, B., Rosenthal, S., Serago, C. & Urie, M. (1996) A pencil beam algorithm for proton dose calculations. *Phys. Med. Biol.*, **41**, 1305-1330.
- Jiang, H., Seco, J. & Paganetti, H. (2007) Effects of Hounsfield number conversion on CT based proton Monte Carlo dose calculations. *Med. Phys.*, **34**, 1439-1449.
- Johansson, S., Svensson, H. & Denekamp, J. (2002) Dose response and latency for radiation-induced fibrosis, edema, and neuropathy in breast cancer patients. *Int. J. Radiat. Oncol. Biol. Phys.*, **52**, 1207-1219.
- Kadoya, N., Obata, Y., Kato, T., Kagiya, M., Nakamura, T., Tomoda, T., Takada, A., Takayama, K. & Fuwa, N. (2011) Dose-volume comparison of proton radiotherapy and stereotactic body radiotherapy for non-small-cell lung cancer. *Int. J. Radiat. Oncol. Biol. Phys.*, **79**, 1225-1231.
- Kanai, T., Kanematsu, N., Minohara, S., Komori, M., Torikoshi, M., Asakura, H., Ikeda, N., Uno, T. & Takei, Y. (2006) Commissioning of a conformal irradiation system for heavy-ion radiotherapy using a layer-stacking method. *Med. Phys.*, **33**, 2989-2997.
- Kanemoto, A., Mizumoto, M., Okumura, T., Takahashi, H., Hashimoto, T., Oshiro, Y., Fukumitsu, N., Moritake, T., Tsuboi, K., Sakae, T. & Sakurai, H. (2013) Dose-volume histogram analysis for risk factors of radiation-induced rib fracture after hypofractionated proton beam therapy for hepatocellular carcinoma. *Acta Oncol.*, **52**, 538-544.
- Matsuda, A., Matsuda, T., Shibata, A., Katanoda, K., Sobue, T. & Nishimoto, H.; The Japan Cancer Surveillance Research Group (2013) Cancer incidence and incidence rates in Japan in 2008: a study of 25 population-based cancer registries for the Monitoring of Cancer Incidence in Japan (MCIJ) project. *Jpn. J. Clin. Oncol.*, **44**, 388-396.
- McGarry, R.C., Papiez, L., Williams, M., Whitford, T. & Timmerman, R.D. (2005) Stereotactic body radiation therapy of early-stage non-small-cell lung carcinoma: Phase I study. *Int. J. Radiat. Oncol. Biol. Phys.*, **63**, 1010-1015.
- Moyers, M.F., Miller, D.W., Bush, D.A. & Slater, J.D. (2001) Methodologies and tools for proton beam design for lung tumors. *Int. J. Radiat. Oncol. Biol. Phys.*, **49**, 1429-1438.
- Mutter, R.W., Liu, F., Abreu, A., Yorke, E., Jackson, A. & Rosenzweig, K.E. (2012) Dose-volume parameters predict for the development of chest wall pain after stereotactic body radiation for lung cancer. *Int. J. Radiat. Oncol. Biol. Phys.*, **82**, 1783-1790.
- Nagata, Y., Takayama, K., Matsuo, Y., Norihisa, Y., Mizowaki, T., Sakamoto, T., Sakamoto, M., Mitsumori, M., Shibuya, K., Araki, N., Yano, S. & Hiraoka, M. (2005) Clinical outcomes of a phase I/II study of 48 Gy of stereotactic body radiotherapy in 4 fractions for primary lung cancer using a stereotactic body frame. *Int. J. Radiat. Oncol. Biol. Phys.*, **63**, 1427-1431.
- Nambu, A., Onishi, H., Aoki, S., Tominaga, L., Kuriyama, K., Araya, M., Saito, R., Maehata, Y., Komiyama, T., Marino, K., Koshiishi, T., Sawada, E. & Araki, T. (2013) Rib fracture after stereotactic radiotherapy for primary lung cancer: prevalence,

- degree of clinical symptoms, and risk factors. *BMC Cancer*, **13**, 68.
- Nirula, R. & Mayberry, J.C. (2010) Rib fracture fixation: controversies and technical challenges. *Am. Surg.*, **76**, 793-802.
- Paganetti, H., Jiang, H., Parodi, K., Slopesma, R. & Engelsman, M. (2008) Clinical implementation of full Monte Carlo dose calculation in proton beam therapy. *Phys. Med. Biol.*, **53**, 4825-4853.
- Pettersson, N., Nyman, J. & Johansson, K.A. (2009) Radiation-induced rib fractures after hypofractionated stereotactic body radiation therapy of non-small cell lung cancer: a dose- and volume-response analysis. *Radiother. Oncol.*, **91**, 360-368.
- Richardson, J.D., Franklin, G.A., Heffley, S. & Seligson, D. (2007) Operative fixation of chest wall fractures: an underused procedure? *Am. Surg.*, **73**, 591-597.
- Shirata, Y., Jingu, K., Koto, M., Kubozono, M., Takeda, K., Sugawara, T., Kadoya, N. & Matsushita, H. (2012) Prognostic factors for local control of stage I non-small cell lung cancer in stereotactic radiotherapy: a retrospective analysis. *Radiat. Oncol.*, **7**, 182.
- Stephans, K.L., Djemil, T., Tendulkar, R.D., Robinson, C.G., Reddy, C.A. & Videtic, G.M. (2012) Prediction of chest wall toxicity from lung stereotactic body radiotherapy (SBRT). *Int. J. Radiat. Oncol. Biol. Phys.*, **82**, 974-980.
- Taremi, M., Hope, A., Lindsay, P., Dahele, M., Fung, S., Purdie, T.G., Jaffray, D., Dawson, L. & Bezjak, A. (2012) Predictors of radiotherapy induced bone injury (RIBI) after stereotactic lung radiotherapy. *Radiat. Oncol.*, **7**, 159.
- Timmerman, R., McGarry, R., Yiannoutsos, C., Papiez, L., Tudor, K., DeLuca, J., Ewing, M., Abdulrahman, R., DesRosiers, C., Williams, M. & Fletcher, J. (2006) Excessive toxicity when treating central tumors in a phase II study of stereotactic body radiation therapy for medically inoperable early-stage lung cancer. *J. Clin. Oncol.*, **24**, 4833-4839.
- Welsh, J., Thomas, J., Shah, D., Allen, P.K., Wei, X., Mitchell, K., Gao, S., Balter, P., Komaki, R. & Chang, J.Y. (2011) Obesity increases the risk of chest wall pain from thoracic stereotactic body radiation therapy. *Int. J. Radiat. Oncol. Biol. Phys.*, **81**, 91-96.
- Xia, T., Li, H., Sun, Q., Wang, Y., Fan, N., Yu, Y., Li, P. & Chang, J.Y. (2006) Promising clinical outcome of stereotactic body radiation therapy for patients with inoperable Stage I/II non-small-cell lung cancer. *Int. J. Radiat. Oncol. Biol. Phys.*, **66**, 117-125.
-